A NEW DEM RECONSTRUCTION METHOD BASED ON AN ACCURATE FLATTENING ALGORITHM IN INTERFEROMETRIC SAR

Zheng Xiang, Kaizhi Wang and Xingzhao Liu, *IEEE Member*

Department of Electronic Engineering, Shanghai Jiao Tong University
800 Dongchuan Road, Min Hang, Shanghai, China
phone: +86 021-34205435, email: xiangzheng@sjtu.edu.cn

ABSTRACT

This paper presents a new approach to reconstruct digital elevation model (DEM) without compensating the flat earth phase back to the unwrapped interferometry in the Interferometric Synthetic Aperture Radar (InSAR). The new approach is based on an accurate flattening algorithm called model-spectrum algorithm which combines the advantages of classic algorithms. The experimental results show that the new algorithm has a better performance than the conventional ones. Based on this novel algorithm, DEM reconstruction can be implemented by a quasi-linear scaling after phase unwrapping. There is no need to add the flat earth phase back to the flattened interferogram, which avoids complex geometrical conversion as what is done in the conventional algorithms.

Index Terms **—** Interferometric Synthetic Aperture Radar, Flattening, Interferogram, Digital Elevation Model, Parameter estimation

1. INTRODUCTION

Interferometric Synthetic Aperture Radar (InSAR) technique is widely used in many fields such as surveying topography, estimating ocean's currents, detecting and locating moving targets, and so on. Basic InSAR processing flow can be concluded as follows [1]: selecting image couple for interferometry, co-registering images, generating interferogram, flattening interferogram, filtering noise, unwrapping phase, reconstructing digital elevation model (DEM). Among these steps, the flattening interferogram process (i.e., flat-earth-removal) imposes great influence on InSAR processing and there are mainly two kinds of algorithms. The first kind is based on parametric models [2] or DEM data [3]. It requires a lot of high-precision geometrical information or referenced DEM. The second kind is based on the estimation from interferogram[1]. This algorithm (max-spectrum algorithm) is widely used in many InSAR processors, but it supposes that the parallel baseline does not change along the range direction.

Generally speaking, these two existing kinds of flattening algorithms can not obtain an accurate flat earth phase due to lack of information or roughness of models. The inaccurate flattening result always leads to an additional compensation on the unwrapped phase by adding back the flat earth phase into the interferogram [4]. It seems that the purpose of the conventional flattening algorithms is to wipe out most of the flat earth phase and decreases the density of fringes in the interferogram. Once the density of the interferogram (i.e., the discontinuity of the phase) is reduced, phase unwrapping will become much easier. It is obviously a waste of time and resource to first subtract and then add the flat earth phase, but unfortunately this seemingly redundant processing is necessary due to an inaccurate flat earth phase.

In this paper, a novel algorithm called model-spectrum is proposed to calculate the flat earth phase accurately. An elaborated model of flat earth phase is built and the spectrum of interferogram is used to optimize parameters of the model. Compared with the common algorithms, fewer system parameters are required and more available resources are exploited in this algorithm. The flattened interferogram reflects basically the DEM. Then we need not add the flat earth phase back into the interferogram and the DEM reconstruction is directly implemented on the phase by a quasi-linear scaling. In Section 2, the theoretical analysis of the cross-track InSAR flat earth effects is first discussed, and the model-spectrum algorithm to estimate the flat earth phase is presented. The DEM reconstruction based on the flattened interferometric phase is also analyzed. In Section 3, the new proposed algorithm of flat-earth-removal is tested by the data from an airborne InSAR system and the DEM is generated according to the analysis in the previous section. The result from one of the conventional algorithm (max-spectrum algorithm) is tested for comparison. Meanwhile some discussion is made in this section. Finally a conclusion is drawn in Section 4.

2. ANALYSIS OF FLATTENING AND DEM RECONSTRUCTION

Flat-earth-removal and DEM reconstruction are two separated steps among InSAR processing. In the following contents, they are analyzed and a bridge between them is built based on an accurate flattening algorithm.

2.1. Accurate flat earth phase removal

The interferometric phase φ varies with the location of the targets since the two antennae in a cross-track InSAR system have different look angles to the targets on the ground. It can be expressed as the sum of targets' topography phase φ_{topo}, flat earth phase φ_{earth}, and φ_{others}, which is responsible to any other phase variation. The purpose of flat-earth-removal is to remove φ_{earth} in the interferogram. In the cross-track mode only the flat earth effects in the range direction needs to be considered. Figure 1 illustrates the geometry of an airborne cross-track InSAR system.

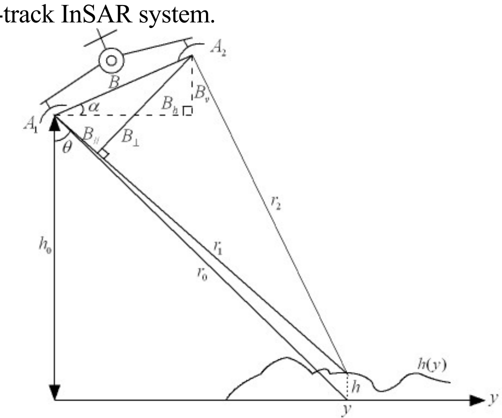

Figure 1: Geometry of InSAR system

In figure 1, θ is the incident angle, α is the tilt angle, r_1 and r_2 are the distance between the two antennae and a point target on the terrain, h_0 is the height of the aeroplane. The baseline B can be decomposed into the horizontal baseline B_h and the vertical baseline B_v, or the perpendicular baseline $B_\perp$ and the parallel baseline $B_{//}$. The flat earth phase can be expressed as:

$$\varphi_{earth} = \frac{2\pi}{\lambda}\left(r_2 - r_1\right)\Big|_{h=0} \approx -\frac{2\pi}{\lambda} B\sin\left(\theta-\alpha\right) = -\frac{2\pi}{\lambda} B_{\|}, \quad (1)$$

where λ is the wavelength and

$$r_1 = \sqrt{y^2 + \left(h_0 - h\right)^2}, \quad (2)$$

$$r_2 = \sqrt{\left(y - B_h\right)^2 + \left(h_0 + B_v - h\right)^2}. \quad (3)$$

From (1) some conclusions can be yielded: The flat earth phase is approximately only dependent on the parallel baseline $B_{//}$ or the incident angle θ. Meanwhile, the 2π fixed interval of the wrapped flat earth phase φ_{earth} makes the corresponding θ behave as "dense at near range while loose at far range" due to the nonlinearity of the sinusoidal function in (1).

Let the incident angle $\theta \in [\theta_{\min}, \theta_{\max}]$ along the range direction, then:

$$\Delta\varphi = -\frac{2\pi B}{\lambda}\left(\sin\left(\theta_{\max}-\alpha\right) - \sin\left(\theta_{\min}-\alpha\right)\right), \quad (4)$$

where $\Delta\varphi$ is the phase difference between the near and far range. Then the tile angle α can be calculated from (4):

$$\alpha = \frac{\theta_{\max}+\theta_{\min}}{2} - \arccos\left(\frac{-\lambda\cdot\Delta\varphi}{4\pi B\sin\left(\left(\theta_{\max}-\theta_{\min}\right)/2\right)}\right). \quad (5)$$

Once the baseline's tilt angle α is calculated, the unwrapped flat earth phase can be obtained easily by using (1).

To calculate the tilt angle α from (5), the phase difference $\Delta\varphi$ must be estimated firstly. The phase-jumps (jumps from π to $-\pi$ or in reverse caused by phase discontinuity) of the interferometric fringes along the range direction can be easily detected in the interferogram (i.e., N_1). Then the phase difference $\Delta\varphi$ can be expressed as below:

$$\Delta\varphi = \left(\left(N_1 - 1\right) + N_2\right)\cdot 2\pi, \qquad N_2 \in \left(0, 2\right), \quad (6)$$

where N_2 is the percentage of 2π at both the near and far range in the interferometric phase. Meanwhile, if the flat earth phase can be removed from the interferogram accurately, the flattened interferogram will be consistent basically with the topography which does not vary greatly. So the main energy of flattened interferogram's spectrum will concentrate at the zero-frequency and form a sharp pulse in the range direction. From this point, the choices of N_2 must make the flattened interferogram's spectrum have a peak value at the zero-frequency position, and among these choices the optimal one should lead to the sharpest pulse. So the method to optimize the value of N_2 is summarized as follows:

Step 1: For every test value of N_2, the FFT is operated on the interferogram $\varphi_{M\times N}$ row by row (along the range direction), and the results are averaged to avoid the influence by noises [4]:

$$\mathbf{\Phi}[1:N] = \sum_{i=1}^{M} \mathrm{FFT}\left[\varphi[1:N]\right]. \quad (7)$$

Step 2: Then the choices of N_2 which lead to a peak value of $\mathbf{\Phi}(n)$ at the zero-frequency are restored.

Step 3: Among these restored N_2, the optimal one should lead to the sharpest pulse formed by $\mathbf{\Phi}(n)$ in (8). The sharpness is measured by the peak-side-lobe-ratio (PSLR): the ratio of the peak value and the largest value around the peak in tenfold sample interval Δn [4]:

$$\mathrm{PSLR} = 10\lg\left(\max_{|n|<\Delta n}\left(\mathbf{\Phi}^2(n)\right) / \max_{\Delta n<|n|<5\Delta n}\left(\mathbf{\Phi}^2(n)\right)\right). \quad (8)$$

Once N_2 is determined, the flat earth phase can be easily obtained by (1), (5) and (6).

Some theoretical comparison with the conventional algorithms is discussed. Two categories of flattening algorithms have been introduced in section 1. The first type calculates the flat earth phase in terms of geometrical parameters, otherwise fit the expression by a polynomial from known DEM. However in many cases such reliable parameters or reference DEM are usually absent. The second type computes the flat earth phase by measuring the dominant fringe frequency in the range direction of the interferometry and introducing into the corresponding linear phase compensation. This algorithm may be more reasonable if it considered the following two: one is that only an integer of dominant fringes can be measured, and the other is that the linear phase compensation has comparatively big errors corresponding to the nonlinearity in (1). Obviously the first type is only dependent on the external information without the assistance from the interforometry itself, while the second type is in reverse. In our flattening algorithm, both the model of the cross-track InSAR and the spectrum of complex interferogram are exploited to remove the flat earth phase accurately.

2.2. DEM reconstruction on flattened interferogram

In figure 1, the topography phase φ_{topo} in cross-track InSAR by Taylor expansion (2) and (3) is:

$$\begin{aligned}\varphi_{topo} &= \varphi - \varphi_{earth} \\ &= \frac{2\pi}{\lambda}\left(\frac{B_v}{2r_0^3}h^3 - \frac{8h_0B_v + 4B_v^2 + 2M}{8r_0^3}h^2 + \frac{MB_v + \mathbf{h_0M - 2B_vr_0^2}}{\mathbf{2r_0^3}}\mathbf{h} + \mathrm{O}\left(\frac{1}{r_0^6}\right)\right), \quad (9)\end{aligned}$$

where φ is the original interferometric phase, $r_0 = \sqrt{y^2 + h_0^2}$ and $M = -2yB_h + B^2 + 2h_0B_v$.

Attention may be paid to that there is no approximation in the derivation until now. If the numerical terms higher than $\mathrm{O}(1/r_0)$ is ignored, only the bold type in (9) remains and it is simplified as:

$$\varphi_{topo} \approx \frac{2\pi}{\lambda}\frac{-h_0yB_h + h_0^2B_v - B_vr_0^2}{r_0^3}h = \frac{-2\pi B_\perp y}{\lambda r_0^2}h\,. \quad (10)$$

So,

$$h \approx \frac{-\lambda}{2\pi B_\perp}\frac{h_0^2 + y^2}{y}\varphi_{topo}\,. \quad (11)$$

From (11), the importance of $B_\perp$ can be concluded clearly: the effective contribution of baseline to topographical surveying is mainly focus on its perpendicular component. Meanwhile equation (11) explains the relationship between the precision of surveying and system parameters: if wavelength λ is shorter and ground distance y is nearer, the precision of topographical surveying is improved. Equation (11) also expounds that the height h is linear to the flattened phase φ_{topo} by engineering approximation when the variety of ground distance y is much smaller than the value itself.

To calculate the transform from flattened phase to terrain's height in (11), $B_\perp$ is still unknown and it can be computed by the imaging parameters. But in practical situation the precision of parameters is limited and other approaches to calculate $B_\perp$ are required. In [5], the author related $B_\perp$ with the spectral shift Δf that corresponds to the phase gradient and to the fringe frequency. This method adopts some numerical approximation and the result is not so satisfying. In the previous part, when the flat earth phase is estimated by the model-spectrum algorithm, the tile angle α is obtained at the same time. Meanwhile the terrain's height calculated by (11) is a relative value which reflects the relative difference of height. A constant value of height h_{const} must be added in (11) as to get the absolute height of the terrain. So the DEM can be calculated as follows:

$$h \approx \frac{-\lambda}{2\pi\sin\left(\pi/2 - \theta + \alpha\right)}\frac{h_0^2 + y^2}{y}\varphi_{topo} + h_{const}\,, \quad (12)$$

where α is computed by (5) and h_{const} is estimated by one reference DEM on the ground. From the analysis above, after phase filtering and unwrapping, the DEM can be directly calculated on the accurately flattened interferogram by a quasi-linear scaling.

3. APPLICATION AND DISCUSSION

Two sets of SAR data from a mountainous area in North China are collected by an airborne dual-antenna cross-track InSAR. Figure 2(a) is the SAR image from the master antenna. Figure 2(b) shows the interferometric phase of the master and slave image after co-registration where the property of "dense at near range while loose at far range" is clearly. The result of max-frequency algorithm is shown in figure 2(c). The model-spectrum algorithm works as follows: By detecting the interferogram, the number of phase-jumps N_1 is 6 (as the dark lines in figure 2(b)). Then N_2 is searched in the bound (0, 2) by a step of 0.1 and N_2=0.4 of peak at zero-frequency position and maximum PSLR=256.4 is selected according to the method in this algorithm. The tile angle α=-30.4135° is incidentally obtained. The flattened interferogram by the new algorithm is illustrated in figure 2(d).

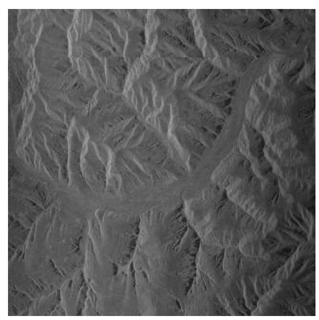

(a) SLC master image

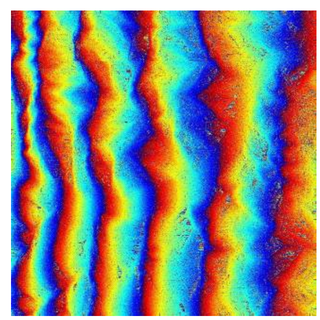

(b) Interferometric phase

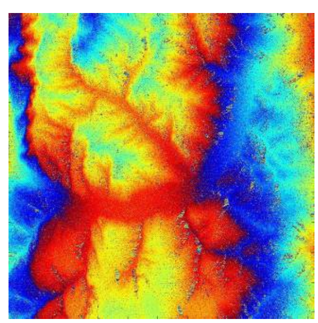

(c) Max-frequency algorithm

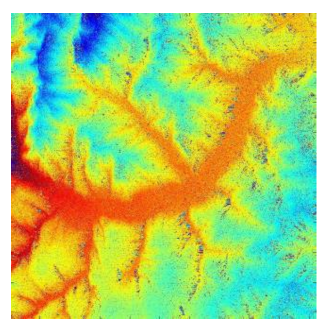

(d) Model-spectrum algorithm

Figure 2: Real data results, where horizontal axis is the range direction and vertical the azimuth

The two results in figure 2(c) and figure 2(d) are compared and some comments are made: The max-frequency algorithm totally failed at the far and near range, while it seems successful at the middle range position. The reason of this phenomenon is that the max-frequency algorithm does not consider the variety of parallel baseline along the range direction (or the property of "dense at near range while loose at far range" of the interferometric phase), and the flat earth phase with aequilate wrappings only matches the trend of interferometric fringes at the middle location where there is a country road, but fails at the near and far position. The model-spectrum gets a much better flattened result and totally eliminates the sidelong fringes caused by the flat earth effects. Along with the accurate removal of flat earth phase, a lot of phase discontinuities, except some noises in small regions caused by radar shadow and etc, are eliminated and this brings much convenience to the phase unwrapping.

Then the flattened interferogram is filtered and unwrapped, and the final DEM result is calculated by (12) and demonstrated in figure 3. The value of h_{const} is supposed to be compute by one of the reference DEM on the ground, while several points are selected to obtain a high-precision constant height. The final averaged value of h_{const} is 801.3m.

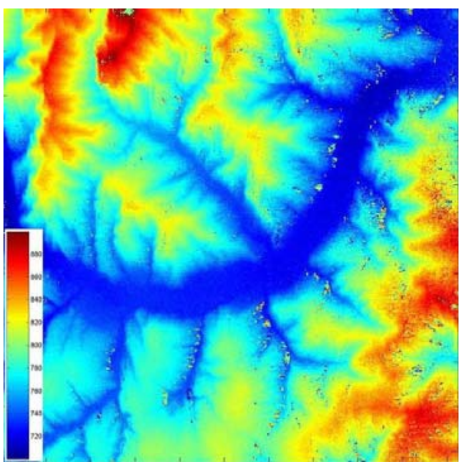

Figure 3: Final DEM reconstruction result

4. CONCLUSION

In this paper, the flat earth effects and DEM reconstruction based on accurate flattening is analyzed firstly. For the cross-track InSAR flattening, a new algorithm is given and called model-spectrum algorithm. This new algorithm builds a model of flat earth effects and uses the spectrum of interferogram to optimize some parameters in the model. Then the model-spectrum algorithm is tested by real interferometric data, and compared with the results by the max-frequency algorithm. The experimental results show that the model-spectrum algorithm is more effective in wiping off flat earth phase than the max-frequency algorithm. If the flat earth phase is totally removed from the interferogram, a quasi-linear scaling can be implemented on the interferogram to get the DEM. This avoid adding back the flat earth phase back to the interferogram and deriving complex geometrical relationships as in general practice.

Lastly, the flat-earth-removal and DEM reconstruction in InSAR processing is concluded as follows: this model-spectrum algorithm proposed in this paper is based on both a simplified model of flat earth effects and the spectrum of interferogram. It provides more satisfied flattening results than the max-frequency algorithm, while require less system parameters or DEM information than the algorithms based on parametric models or DEM data. Moreover some parameters calculated by this algorithm are used in the DEM reconstruction. Since the flat earth phase computed by this new flattening algorithm has high degree of accuracy, only a quasi-linear transition is required when transferring phase to height. In the further study, the influence of geodetic curvature to flat-earth-removal should also be considered [6], though it has not been analyzed in this paper. Meanwhile, the radar shadow is also a serious problem in DEM reconstruction of mountainous terrain as the interferometric phase of shadow regions are random and cause much inconvenience to the phase unwrapping [7]. It is necessary to take all these issues into consideration in flat-earth-removal and DEM reconstruction of SAR interferometry.

REFERENCE

[1] J. Moreira, M. Schwäbisch, G. Fornaro, R. Lanari, R. Bamler, D. Just, U. Steinbrecher, H. Breit, M. Eineder, G. Franceschetti, D. Geudtner, and H. Rinkel, "X-SAR interferometry: First results," IEEE Trans. Geosci. Remote Sensing, vol. 33, no. 4, pp. 950-956, Jul. 1995.

[2] C. Prati, F. Rocca, "Limits to the resolution of elevation maps from stereo SAR images," *Int. J. Remote Sensing*, vol. 11(12), pp. 2215-2235, December 1990.

[3] K. Ren, V. Prinet, and X. Shi, "Spaceborne InSAR flat earth removal processing based on geolocation method," *Geomatics and Information Science of Wuhan University*, vol. 28(3), pp. 326-329, June 2003.

[4] S. S. Hartley. System design document of C-SAR. Technique report of C-SAR, May 1995.

[5] D. Mu, Z.D. Zhu, H.C. Zhang, "Study on interforometric SAR 3-D dimensional remote sensing," Remote Sensing Technology and Application," vol. 15, no. 4, Dec. 2000.

[6] Q. Zeng, X. Li, and L. Gao, "An improvement to flattening in interferometric SAR processing," *Proceedings of SPIE – The International Society for Optical Engineering* 6200, art. No. 6200D, 2006.

[7] M. Eineder and S. Suchandt, "Recovering radar shadow to improve interferometric phase unwrapping and DEM reconstruction," *IEEE Trans. Geosci. Remote Sensing*, vol. 41, pp. 2959-2962, December 2003.